Werk

Jahr: 1981
Kollektion: fid.geo
Signatur: 8 Z NAT 2148:49
Digitalisiert: Niedersächsische Staats- und Universitätsbibliothek Göttingen
Werk Id: PPN1015067948_0049
PURL: http://resolver.sub.uni-goettingen.de/purl?PPN1015067948_0049

LOG Id: LOG_0054
LOG Titel: Extremal models for electromagnetic induction in two-dimensional perfect conductors
LOG Typ: article

Übergeordnetes Werk

Werk Id: PPN1015067948
PURL: http://resolver.sub.uni-goettingen.de/purl?PPN1015067948
OPAC: http://opac.sub.uni-goettingen.de/DB=1/PPN?PPN=1015067948

Contact

Niedersächsische Staats- und Universitätsbibliothek Göttingen
Georg-August-Universität Göttingen
Platz der Göttinger Sieben 1
37073 Göttingen
Germany
Email: gdz@sub.uni-goettingen.de

J Geophys (1981) 49:217–225

Journal of Geophysics

Extremal Models for Electromagnetic Induction in Two-Dimensional Perfect Conductors

P. Weidelt

Bundesanstalt für Geowissenschaften und Rohstoffe, Stilleweg 2, D-3000 Hannover 51, Federal Republic of Germany

Abstract. The simple problem of electromagnetic induction in two-dimensional perfect conductors is considered. Extremal models are constructed maximizing the depth to the top of the conductor for magnetic field data at $N=1$ or 2 observation points. It is assumed that the inducing magnetic field is quasi-uniform and that the electromagnetic field is excluded from a depth greater than $z=A$, where A is prescribed. Then the extremal models consist of two levels: a conducting plane at a depth $z=A$ and either N conducting strips or N gaps in a conducting plane at a depth $z=z_0$, which is the maximum possible depth as calculated from the data. The problem is solved by conformal mapping and illustrated by data from the North German conductivity anomaly.

Key words: Electromagnetic induction – Maximum depth rule – Conformal mapping – North German conductivity anomaly

1 Introduction

Now that techniques have been developed for estimating by various kinds of generalized matrix inversion the degree of non-uniqueness of a given imperfect data set, interest has arisen in the problem of how to obtain geophysically relevant properties common to all models, which both fit the data and satisfy certain a priori assumptions (i.e., the feasible models). The research of Parker on ideal bodies is a typical example of this approach (Parker 1972, 1974, 1975). Work along similar lines has been carried out by Sabatier (1977a–c), Safon et al. (1977), Rietsch (1978), Huestis (1979), and Barcilon (1979). The investigation of the upper bound of a minimum value (or the lower bound of a maximum value) of a special model parameter has been of particular importance in this development. For instance, if a data set is to be interpreted in terms of a buried structure, then any feasible model has a minimum depth of burial (the depth to the top of the structure). If we could find the model with the greatest minimum depth of burial, then the minimum depth of burial of all feasible models cannot be greater than this upper bound. The search for the maximum depth of the top of a buried structure leads to maximum depth rules. For potential field data many rules of this nature have been established (Bott and Smith 1958; Smith 1959, 1960).

In this paper maximum depth rules are derived for the simplest problem in electromagnetic induction, where the model is two-dimensional and consists only of perfect conductors and insulators, thus admitting a treatment by conformal mapping. In this limit the surface of the conductor coincides with a field line, since the magnetic field component normal to the conductor vanishes. The following problem is considered: Assume cartesian coordinates y, z (z positive downwards, surface at $z=0$) and a quasi-uniform inducing field in y-direction. Further, assume that the perfect conductor extends with horizontal tangents to infinity and that it excludes the electromagnetic field from a depth greater than $z=A$, where A is known or can be estimated. The magnetic field components $H_y(p)$ and $H_z(p)$, normalized by H_n, the horizontal magnetic surface field for $y\to\pm\infty$, are given at a surface point p

$$h_y=H_y(p)/H_n, \qquad h_z=H_z(p)/H_n \tag{1.1}$$

The problem is to determine the conductor with the deepest top complying with h_y, h_z and A.

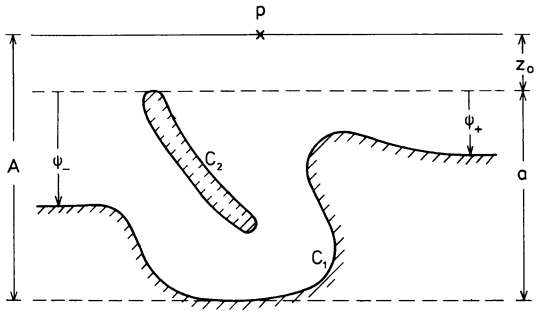

Fig. 1. The model under consideration. C_1 and C_2 are the surfaces of perfect conductors. The other symbols are explained in the text

A section across the most general model under consideration is shown in Fig. 1. It consists of a perfect conductor with undulating interface C_1 extending to infinity and a second isolated conductor with boundary C_2. It turns out that a doubly connected conductor is necessary to construct extremal models for all possible values of h_y and h_z. Fig. 1 introduces z_0 as the depth to the top of the conductor and $a=A-z_0$ as the depth range of irregular distribution of conducting material. The horizontal asymptotes of C_1 lie at depths $\psi_\pm$ below z_0.

The above problem is solved for a single observation point p in Sect. 2, and partial results for two observation points are presented in Sect. 3. Finally, in Sect. 4, the findings are applied to real data.

0340-062X/81/0049/0217/$01.80

2 Single-Point Extremal Models

2.1 Simply Connected Conductors

For ease of presentation we first search for extremal models within the class of simply connected conductors, restricting attention to the undulating interface C_1. Let

$$p=y-i(z-z_0) \quad \text{and} \quad w=u+iv \tag{2.1}$$

be two complex variables and let $p(w)$ map the line $v=0$ conformally into the interface C_1 and the half-plane $v>0$ into the insulator above C_1. Let this mapping be normalized by

$$p'(w)\to 1 \quad \text{for} \quad w\to\infty,\ v>0 \tag{2.2}$$

The parameter representation of C_1 is

$$p(w)=y(u)-i\psi(u) \quad \text{for} \quad -\infty<u<+\infty,\ v=0 \tag{2.3}$$

where $\psi=z-z_0$ is subject to $0\leqq\psi(u)\leqq a$ with $a=A-z_0$ (Fig. 1). The function $\psi(u)$ with $\psi=z-z_0$ and $a=A-z_0$ (Fig. 1). The function $\psi(u)$ with the limiting values $\psi_\pm$ for $u\to\pm\infty$ is the boundary value of the negative imaginary part of $p(w)$. The function $p(w)$ is analytic in $v>0$ and satisfies Eq. (2.2). Hence,

$$p(w)=w+\frac{1}{\pi}(\psi_+-\psi_-)\log w-\frac{1}{\pi}\int_{-\infty}^{+\infty}\frac{\tilde{\psi}(t)\,dt}{t-w} \tag{2.4}$$

where

$$\tilde{\psi}(u)=\begin{cases}\psi(u)+\psi_+-\psi, & u<0\\ \psi(u), & u>0\end{cases}$$

The subtraction term in $\tilde{\psi}$ and its subsequent reconsideration in the log term is necessary to ensure the convergence of Eq. (2.4) if $\psi_+\neq\psi_-$. Using the identity

$$\operatorname{Im}\left\{\lim_{v\to+0}\frac{1}{\pi}\int_{-\infty}^{+\infty}\frac{\tilde{\psi}(t)\,dt}{t-w}\right\}=\tilde{\psi}(u)$$

it is easily verified that Eq. (2.4) meets all requirements. The normalized magnetic field in the p-plane,

$$h=h_y+ih_z=(H_y+iH_z)/H_n \tag{2.5}$$

is derived from a normalized complex potential $f(p)$ by $h(p)=f'(p)$ where, by virtue of the Cauchy-Riemann differential equations, the lines $\operatorname{Re}f=\text{const.}$ are the equipotential lines and the lines $\operatorname{Im}f=\text{const.}$ the field lines. By the conformal mapping $w(p)$ this field is mapped into a magnetic field in the w-plane, which is derived from the complex potential $g(w)=f(p)$. In view of the quasi-uniform inducing field the magnetic field in the upper w-halfplane is also uniform and can be derived from the normalized complex potential $g(w)=w$, where Eq. (2.2) has been used. Hence the magnetic field in the p-plane is simply

$$h(p)=f'(p)=g'(w)\,w'(p)=1/p'(w) \tag{2.6}$$

or expressing h by means of Eq. (2.4) in terms of ψ,

$$\frac{1}{h}=1-\frac{1}{\pi}\int_{-\infty}^{+\infty}\frac{\psi(t)\,dt}{(t-w)^2} \tag{2.7}$$

For computational ease it is temporarily assumed that instead of A the quantity a is prescribed. We are then faced with the following problem:

The normalized complex magnetic field h and the depth range a are given. Determine the complex point w and the real function $\psi(u)$ with $0\leqq\psi\leqq a$, which maximizes $z_0=\operatorname{Im}p(w)$ subject to Eq. (2.7). Moreover, for $v\geqq 0$ $p(w)$ has to be a univalent (or one-to-one) mapping.

This problem of constrained maximization is best solved by the use of Lagrangian multipliers (Luenberger 1969, p. 249), yielding, for the minimization of $-z_0$ (to retain the canonical form), the Lagrange function

$$L=\operatorname{Im}\{-p(w)+\lambda[p'(w)-1/h]\}-\int_{-\infty}^{+\infty}\mu^-(t)\,\psi(t)\,dt+\int_{-\infty}^{+\infty}\mu^+(t)(\psi(t)-a)\,dt \tag{2.8}$$

The complex multiplier $\lambda=\lambda_y+i\lambda_z$, where λ_y and λ_z are unrestricted in sign, is associated with the equality constraint Eq. (2.7). On the other hand, the functions $\mu^-(t)$ and $\mu^+(t)$ associated with the inequalities $-\psi(t)\leqq 0$ and $\psi(t)-a\leqq 0$, respectively, are *positive* where the inequalities are binding (i.e., satisfied with the equality sign), and zero elsewhere. The existence of an extremum requires that the first variation of L with respect to ψ vanishes. Hence,

$$\operatorname{Im}\left\{\frac{1}{\pi(t-w)}-\frac{\lambda}{\pi(t-w)^2}\right\}-\mu^-(t)+\mu^+(t)=0 \tag{2.9}$$

Since L is linear in ψ, this function does not occur in Eq. (2.5). From the fact that $\mu^-=0$ for $\psi>0$ and $\mu^+=0$ for $\psi<a$ it is immediately deduced that the only points t where $\psi(t)$ attains neither its lower nor its upper bound, are the roots of

$$\operatorname{Im}\left\{\frac{1}{t-w}-\frac{\lambda}{(t-w)^2}\right\}=0 \tag{2.10}$$

which has at most two real roots. This is assumed here and verified in a later stage. The origin on the real axis of the w-plane is now fixed by placing the two roots at $t=\pm c$, $c>0$. Hence, either

$$\text{a)}\quad \psi(t)=\begin{cases}a, & |t|<c\\ 0, & |t|>c\end{cases} \tag{2.11a}$$

or

$$\text{b)}\quad \psi(t)=\begin{cases}0, & |t|<c\\ a, & |t|>c\end{cases} \tag{2.11b}$$

These two cases will be discussed below. The model parameters w and c are determined from the fact that at an extremum the three partial derivatives of

$$L=\operatorname{Im}\{-p(w)+\lambda[p'(w)-1/h]\}$$

with respect to u, v and c have to vanish. This latter form of L differs from Eq. (2.8) by the inequality terms, which vanish for a choice of $p(w)$ according to Eq. (2.11a, b). An analytic function $f(w)$ satisfies

$$\partial_u\operatorname{Im}f(w)=\operatorname{Im}f'(w), \qquad \partial_v\operatorname{Im}f(w)=\operatorname{Re}f'(w)$$

where $\partial_u=\partial/\partial_u$, etc. Hence, the first two conditions are equivalent to

$$-p'+\lambda p''=0 \quad \text{or} \quad \lambda=p'/p'' \tag{2.12}$$

which combined with $\partial_c L=0$ yields the extremal condition

$$\operatorname{Im}\{-\partial_c p+(p'/p'')\,\partial_c p'\}=0 \tag{2.13}$$

Case a:

From Eqs. (2.4) and (2.11a) it follows that

$$p(w)=w+\frac{a}{\pi}\log\left(\frac{-c-w}{+c-w}\right)$$

reducing Eq. (2.13) to

$$\pi(|w|^2-c^2)-2ac=0 \tag{2.14}$$

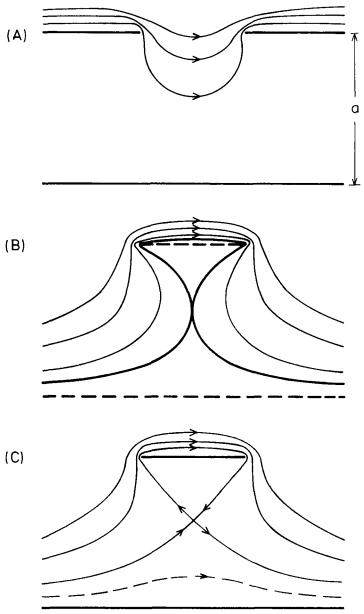

Fig. 2A–C. Types of extremal models for a single observation point showing upper and lower conducting sheets and magnetic field lines: (**A**) for $h_y<1$, (**B**) approximate model for $h_y>1$, (**C**) exact model for $h_y>1$ (see text for full explanation)

Equation (2.14) supplements the complex equation $p'(w)=1/h$. This set of three real equations is solved by

$$u=\frac{a}{\pi}\frac{h_z}{h_y-1}\tan\beta, \quad v=\frac{a}{\pi}\tan\beta, \quad c=\frac{a}{\pi}\frac{2h_y-1}{1-h_y} \tag{2.15a-c}$$

where

$$\tan^2\beta=\frac{2h_y-1}{(h_y-1)^2+h_z^2} \tag{2.16}$$

implying

$$z_0=\operatorname{Im} p(w)=\frac{a}{\pi}(-\beta+\tan\beta)=A\left(1-\frac{\pi}{\pi-\beta+\tan\beta}\right) \tag{2.17}$$

For consistency, insertion of Eq. (2.15a-c) and of λ from Eq. (2.12) will verify that $t=\pm c$ are the two real roots of Eq. (2.10). Equations (2.17) and (2.16) provide a partial answer to the problem under consideration. The answer is incomplete because c, assumed to be positive, becomes negative for $h_y>1$. The second change of sign of c at $h_y=0.5$ is not serious, since the horizontal magnetic field of internal origin, $h_y-0.5$, is always non-negative. (The normal magnetic field H_n consists of the external inducing field and the internal normally induced field in equal parts.)

The type of the extreme model and a few field lines are shown in Fig. 2, part A. It consists of two horizontal halfplanes at $z=z_0$ and a horizontal plane at $z=A$. The width of the gap between the halfplanes (i.e., the distance between the two points where $p'(w)=0$) is

$$d=\frac{2a}{\pi}\left\{\frac{2\varepsilon}{1-\varepsilon^2}+\log\frac{1+\varepsilon}{1-\varepsilon}\right\}, \quad \varepsilon=\sqrt{2h_y-1}$$

For $h_y\to 1-0$ and $h_z>0$ (say), the right halfplane is displaced to infinity, yielding an infinite width.

Case b:

Combining Eqs. (2.4) and (2.11b) we obtain

$$p(w)=w+\frac{a}{\pi}\log\left(\frac{c-w}{c+w}\right) \tag{2.18}$$

and the extremal condition

$$\pi(|w|^2-c^2)+2ac=0$$

The resulting parameters u, v, and z_0 are identical with those given in Eqs. (2.15a, b) and (2.17), whereas

$$c=\frac{a}{\pi}\frac{2h_y-1}{h_y-1}$$

suggests that case b covers the range $h_y>1$. However, an inspection of Eq. (2.18) reveals that $p(w)$ is not univalent for all $v>0$. Only for sufficiently large v are the lines $v=$const., which are field lines for a quasi-uniform inducing field, mapped into the corresponding field lines in the p-plane (Fig. 2, part B). The value of v can decrease until a limiting field line is reached where two different parts of the field line touch at the axis of symmetry. For smaller v, the image of the line $v=$const. has two points of intersection on the axis of symmetry, implying that for $-a\leqq\operatorname{Im} p(w)\leqq 0$ two different points of the w-plane are mapped into the same point of the p-plane. The deepest physically real conductor is traced by the limiting field line, whereas contrary to our assumption the line $v=0$ does not map the interface of a physically real conductor.

Since the search for an extremum model within the restricted class of simply connected conductors failed for $h_y>1$, the broader class of doubly connected conductors will now be considered.

2.2 Doubly Connected Conductors

An account of the theory of conformal mapping of doubly connected domains, which is intimately related to the theory of doubly periodic functions, is given by Koppenfels and Stallmann (1959).

We assume the conductor configuration of Fig. 1: A conductor C_1 with undulating interface extending at both sides, with horizontal tangents, to infinity and an isolated conductor C_2 of finite extent. A very special case of this class is shown at the top of Fig. 3. A branch cut from any point of C_2 to infinity creates a simply connected domain. As in Sect. 2.1 we introduce two complex variables

$$p=y-i(z-z_0), \quad w=u+iv \tag{2.19}$$

where w will now be dimensionless. Using the univalent conformal mapping $w(p)$, the simply connected domain is mapped into a rectangle of length π and heigth $\frac{1}{2}\alpha$ in the w-plane, such that C_1 is mapped into $v=0$ and C_2 into $v=\frac{1}{2}\alpha$, $0\leqq u\leqq\pi$ (top and centre of Fig. 3, for illustration). The aspect ratio of the rectangle depends on the conductor system C_1, C_2. Broadly speaking, α is large if the minimum distance between C_1 and C_2 is large compared with the dimension of C_2, and vice versa. To each physical contour around C_2, which must cross the branch cut, corresponds a *different* rectangle in the w-plane, displaced by a distance π to the right (left) if C_2 was lying to the left (right) of the contour. Hence, $w(p)$ is multi-valued and $p(w)$ periodic, satisfying $p(w+k\pi)=p(w)$ for any integer k.

Let $p=\infty$ be mapped into $w=0$. Then the asymptotic behaviour

$$w(p)=-b/p \quad \text{for } p\to\infty, \ \operatorname{Im} p>0 \tag{2.20}$$

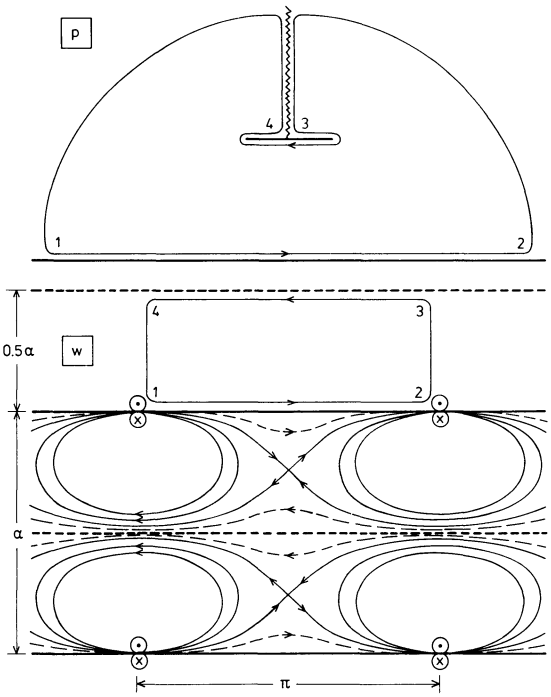

Fig. 3. Example of the mapping of a doubly connected domain in the p-plane (*upper diagram*) onto half a period rectangle in the w-plane (*lower diagram*). The period rectangle is completed by the mirror image at $v=\alpha/2$ and periodically reproduced with periods π and $i\alpha$. The *bottom* shows magnetic field lines for a doubly periodic dipole and a uniform magnetic field in the w-plane. As a consequence of Eq. (2.23) the uniform field is adjusted to yield a vanishing net flux across a line from any point at $v=0$ (except source points) to any point at $v=\alpha/2$. The magnetic field in the w-plane corresponds to a quasi-uniform inducing field in the p-plane

establishes a conformal one-to-one mapping of a neighbourhood of $p=\infty$ onto a neighbourhood of $w=0$, where the scaling length $b>0$ has to be determined. The minus sign ensures that $\mathrm{Im}\, w>0$ if $\mathrm{Im}\, p>0$.

For a quasi-uniform inducing field let

$$H(p)/H_n=h(p)=f'(p), \tag{2.21}$$

where $f(p)$ with $f(p)=p$ for $p\to\infty$ is the normalized complex potential. Then the corresponding normalized potential $g(w)=f(p)$ behaves according to Eq. (2.20) as

$$g(w)=-b/w \quad \text{for } w\to 0, \tag{2.22}$$

which can be interpreted as the potential of a horizontal magnetic dipole or current doublet at $w=0$, corresponding to the fact that the normal magnetic field in the p-plane can be conceived as the limit of a distant line current and its mirror image at C_1.

In virtue of the Cauchy-Riemann differential equations the real part of the complex potential can be interpreted as the ordinary scalar magnetic potential and the imaginary part as the only component of the vector potential. At boundaries to perfect conductors this component vanishes since it is proportional to the time derivative of the electric field, vanishing at conductors. Hence, g satisfies the boundary condition

$$\mathrm{Im}\, g(w)=0 \quad \text{for } v=0 \text{ and } v=\alpha/2 \tag{2.23}$$

The complete potential $g(w)$ can be considered as the superposition of the potentials of the infinite sequence of dipoles a distance π apart along the horizontal axis, plus the potentials of the infinite number of images of this sequence at $v=\alpha$, $-\alpha$, 2α, -2α, ... which ensures that $\mathrm{Im}\, g$ is constant at the conductors at $v=0$ and $v=\alpha/2$, plus the potential of a still unspecified uniform horizontal field which adjusts $\mathrm{Im}\, g$ at both conductors to zero. Hence,

$$g(w)=-b\{\varphi(w,\alpha)+c_1 w+c_2\} \tag{2.24}$$

where

$$\varphi(w,\alpha)=\lim_{M\to\infty}\sum_{m=-M}^{+M}\sum_{k=-\infty}^{+\infty}\frac{1}{w-k\pi-im\alpha}$$

$$=\lim_{M\to\infty}\sum_{m=-M}^{+M}\cot(w-im\alpha) \tag{2.25}$$

$$=\cot w+2\sum_{m=1}^{\infty}\frac{\sin 2w}{\cosh 2m\alpha-\cos 2w} \tag{2.26}$$

$$=\sum_{m=-\infty}^{+\infty}\frac{\sin 2w}{\cosh 2m\alpha-\cos 2w}$$

$$=\vartheta_1'(w)/\vartheta_1(w) \tag{2.27}$$

with

$$\vartheta_1(w)=2\sum_{n=0}^{\infty}(-1)^n e^{-\alpha(n+\frac{1}{2})^2}\sin(2n+1)w \tag{2.28}$$

The above derivations are based on the identities 4.3.91, 4.3.39 and 4.3.31 of Abramowitz and Stegun (1965) and Example 15, Chap. 21 of Whittaker and Watson (1927). In Eq. (2.27) $\vartheta_1(w)$ is the first Theta function for the period ratio $\tau=i\alpha/\pi$ in the notation of Whittaker and Watson. The series (2.26) is rapidly convergent for $\alpha\geqq\pi$. For $\alpha<\pi$ the application of Jacobi's imaginary transformation (Whittaker and Watson 1927, p. 474) to ϑ_1 also yields a rapidly convergent representation:

$$\varphi(w,\alpha)=-\frac{2w}{\alpha}+\frac{\pi}{i\alpha}\varphi\left(\frac{\pi w}{i\alpha},\frac{\pi^2}{\alpha}\right) \tag{2.29}$$

The constants c_1 and c_2 in Eq. (2.24) are determined from the observation that

$$\mathrm{Im}\,\varphi(w,\alpha)=\begin{cases}0, & v=0 \quad \text{(except source points)}\\ -1, & v=\alpha/2\end{cases}$$

The latter result is obtained by rearranging the terms of Eq. (2.25), yielding only a contribution for $m=-M$. Hence, satisfying Eq. (2.23) by $c_1=2/\alpha$, $c_2=0$, we end up with

$$g(w)=-b\{\varphi(w,\alpha)+2w/\alpha\} \tag{2.30}$$

The bottom of Fig. 3 shows a few magnetic field lines, $\mathrm{Im}\, g=\text{const.}$, within a complete period rectangle of length π and height α. A particular feature of the field in any doubly connected domain is the existence of a neutral point ($g'=0$).

The presence of a linear term in the complex potential reflects the fact that the scalar magnetic potential and hence the complex potential is a multi-valued function, increasing after any closed clockwise contour by the amount of current encircled, reckoned positive if flowing in x-direction (into the sheet). Hence, the total current I flowing in the conductor C_2 is

$$I=\frac{2\pi b}{\alpha}H_n \tag{2.31}$$

After having determined $g(w)$, the normalized magnetic field in the p-plane is given by

$$h(p)=f'(p)=g'(w)\cdot w'(p)=g'(w)/p'(w) \tag{2.32}$$

Let $\psi_1(u)$ and $\psi_2(u)$ be the boundary values of the negative imaginary part of $p(w)$ at $v=0$ and $v=\alpha/2$. With the formula of Villat (Koppenfels and Stallmann 1959, p. 107) the mapping function $p(w)$ - analytic in $0<v<\alpha/2$ - is, apart from a real additive constant, given by

$$p(w)=-\frac{1}{\pi}\int_0^\pi \{\psi_1(t)\,\varphi(t-w)-\psi_2(t)\,\chi(t-w)\}\,dt + \frac{2w}{\alpha\pi}\int_0^\pi \{\psi_1(t)-\psi_2(t)\}\,dt \tag{2.33}$$

where

$$\chi(w)=\varphi(w+\tfrac{1}{2}i\alpha)+i=\vartheta_4'(w)/\vartheta_4(w) = \sum_{m=1}^{\infty}\frac{2\sin 2w}{\cosh(2m-1)\,\alpha-\cos 2w} \tag{2.34}$$

using a set of identities given in Chap. 21 of Whittaker and Watson (1927).

Unlike the complex potential $g(w)$, the mapping $p(w)$ is periodic $p(w+\pi)=p(w)$, requiring that the second term of Eq. (2.33) vanishes, i.e.,

$$\int_0^\pi \{\psi_1(t)-\psi_2(t)\}\,dt=0 \tag{2.35}$$

provided that the domain is strictly doubly connected ($\alpha<\infty$).

Because of Eq. (2.20), $p=-b/w$ for $w\to 0$, and

$$\lim_{v\to+0}\frac{1}{\pi}\frac{v}{u^2+v^2}=\delta(u)$$

it is reasonable to split ψ_1 into a bounded part $\tilde{\psi}_1$ and an unbounded part,

$$\psi_1(u)=\tilde{\psi}_1(u)-b\pi\,\delta(u) \tag{2.36}$$

implying that the proper range of integration in Eqs. (2.33) and (2.35) is from -0 to $\pi-0$. For $0\leqq u\leqq\pi$ the functions $\tilde{\psi}_1$ and ψ_2 are bounded by

$$0\leqq\tilde{\psi}_1(u)\leqq a,\qquad 0\leqq\psi_2(u)\leqq a \tag{2.37}$$

where again $a=A-z_0$ (Fig. 1). Hence we are faced with the following problem: The complex number $h=g'(w)/p'(w)$ and the depth range a are given. Determine the two real functions $\tilde{\psi}_1$ and ψ_2, subject to Eq. (2.37), the complex point w and the scale length b such that $z_0=\operatorname{Im} p(w)$ is a maximum.

As in Sect. 2.1, the problem is solved by means of a Lagrange function L, which now reads

$$L=\operatorname{Im}\{-p(w)+\lambda[p'(w)/g'(w)-1/h]\} + \int_0^\pi \{-\mu_1^-\,\tilde{\psi}_1+\mu_1^+(\tilde{\psi}_1-a)-\mu_2^-\,\psi_2+\mu_2^+(\psi_2-a)\}\,dt + \lambda_0\left\{\int_0^\pi(\tilde{\psi}_1-\psi_2)\,dt-\pi b\right\} \tag{2.38}$$

The difference from Eq. (2.8) is only that two functions have to be determined, constrained by Eq. (2.35). Since L is linear in $\tilde{\psi}_1$ and ψ_2, the same arguments as in Sect. 2.1 lead to the result that in an extremal model $\tilde{\psi}_1$ and ψ_2 can attain only the values 0 and a. Since C_2 contours a conductor which does not extend to infinity, ψ_2 must be continuous. The only possible choice is $\psi_2=0$. (In the case $\psi_2=a$ the doubly connected domain degenerates into a simply connected domain, and the results of Sect. 2 can be recovered.) The function $\tilde{\psi}_1(t)$ may have either none or two points of discontinuity, the latter being the roots of

$$\operatorname{Im}\{\varphi(t-w)+\lambda\varphi'(t-w)/g'(w)\}+\pi\lambda_0=0 \tag{2.39}$$

which are mapped into $p=\infty$. First it is assumed that Eq. (2.39) has no roots. Then we have to choose $\tilde{\psi}_1=a$, which implies according to Eqs. (2.35), (2.36) and (2.33) that $b=a$ and

$$p(w)=-a\{\varphi(w)+i\} \tag{2.40}$$

In Eq. (2.33) we have used

$$\int_0^\pi \varphi(t-w)\,dt=\log\vartheta_1(t-w)|_0^\pi=i\pi,\qquad v>0$$

The mapping of Eq. (2.40) maps the line $v=\frac{1}{2}\alpha$ into a horizontal strip at $z=z_0$ and the line $v=0$ into a plane at $z=z_0+a=A$. The model is illustrated in Fig. 2, part C. Inserting Eq. (2.40), the Lagrange function, Eq. (2.38) reduces to

$$L=\operatorname{Im}\{a(\varphi+i)+\lambda[\varphi'/(\varphi'+2/\alpha)-1/h]\}$$

At an extremum, the three partial derivatives with respect to u, v and α vanish. As in Sect. 2.1, the first two admit the elimination of λ, and the third then provides the extremal condition

$$\operatorname{Im}\{\alpha\partial_\alpha\varphi-(\varphi'/\varphi'')\cdot\partial_\alpha(\alpha\varphi')\}=0 \tag{2.41}$$

which supplements the constraint

$$h=1+2/(\alpha\varphi') \tag{2.42}$$

The nonlinear system, Eqs. (2.41) and (2.42) is solved easily by numerical means. Some insight, however, is obtained by an approximate solution. For h_y slightly greater than unity the extremal model must be close to that for $h_y\leqq 1$, i.e., the strip at $z=z_0$ is wide and α is small. In this limit, Eqs. (2.29) and (2.26) yield the approximation

$$\varphi(w,\alpha)=-\frac{2w}{\alpha}+\frac{\pi}{i\alpha}\cot\left(\frac{\pi w}{i\alpha}\right),\qquad \alpha\ll\pi$$

reducing the extremal condition Eq. (2.41) to

$$\cosh\left(\frac{2\pi u}{\alpha}\right)+\left(\frac{\pi^2}{\alpha}-1\right)\cos\left(\frac{2\pi v}{\alpha}\right)=0$$

After solving for u, v, and α, the relationship Eq. (2.17) is reproduced *exactly*. Hence, Eq. (2.17) gives reliable results for $h_y>1$ also if

$$\alpha/\pi^2=(h_y-1)/(2h_y-1)$$

is small. The applicability of Eq. (2.17) for $h_y>1$ is revealed from Fig. 2, parts B and C. The field lines, which become identical at infinity, show a remarkable similarity, except for the different field line topology in the region of weak magnetic fields. The approximation of Eq. (2.17) is worst if both h_y and $|h_z|$ are large, i.e., for points near the edge of the strip. However, the results of Table 1 indicate that for all cases of geophysical interest, Eq. (2.17) provides a completely satisfactory approximation. The figures of Table 1 underline that the search in the extended class of doubly connected conductors consistently yields a slightly greater z_0/A-value than the search in the class of simply connected conductors.

At $h_y=1$ the transition between the extremum models of Fig. 2, parts A and C is continuous: Assuming $h_z>0$, the right edge of the gap (A) tends to $y=+\infty$ for $h_y=1-0$ and the left edge of the strip (C) tends to $y=-\infty$ for $h_y=1+0$.

Table 1. Comparison of approximate and exact z_0/A values

h_y	$\lvert h_z\rvert$	z_0/A (approx.)	z_0/A (exact)
2.0	1.0	0.0973	0.1027
2.0	0.5	0.1494	0.1534
2.0	0.0	0.1790	0.1822
1.5	1.0	0.1036	0.1057
1.5	0.5	0.2213	0.2225
1.5	0.0	0.3371	0.3376

Iso-lines of z_0/A which are circular arcs for $h_y \leqq 1$, are shown in Fig. 4. If only h_y or h_z is given, z_0 is the greatest value attained if the unknown parameter varies freely. If h_y is given, z_0 reaches its maximum for $h_z=0$; if h_z is given the maximum of z_0 occurs on the light dashed line, which in the approximation of Eq. (2.17) is given by $h_z^2=h_y(h_y-1)$.

3 Two-Point Extremum Models

Now we assume that the complex magnetic fields h_1 and h_2 are given at the two surface points p_1 and p_2 with $p_2-p_1=d$, and that the electromagnetic field does not penetrate deeper than a given depth A. From these data we want to obtain the upper bound z_0 of the depth to the top of the anomalous conductivity. For this two-point problem the answer will remain incomplete since for certain combinations of the data triply connected conductors will be required, which cannot be handled with the present tools.

We are going to determine the mapping function $p(w)$, Eq. (2.33), depending on ψ_1 and ψ_2 with $p(w_k)=p_k$, $k=1,2$. The complete Lagrange function is (cf. Eq. (2.38))

$$\begin{aligned} L=\operatorname{Im}\Big\{ & -p_1+\lambda_d(p_2-p_1-d)+\lambda_A(p_1+ia-iA) \\ & +\sum_{k=1}^{2}\lambda_k(p_k'/g_k'-1/h_k)\Big\} \\ & +\int_0^{\pi}\{-\mu_1^-\tilde{\psi}_1+\mu_1^+(\tilde{\psi}_1-a)-\mu_2^-\psi_2+\mu_2^+(\psi_2-a)\}\,dt \\ & +\lambda_0\Big\{\int_0^{\pi}(\tilde{\psi}_1-\psi_2)\,dt-\pi b\Big\} \end{aligned} \tag{3.1}$$

The multiplieers λ_1, λ_2, and λ_d are complex, since each accounts for two constraints, whereas λ_A and λ_0 are real. The length $a=A-z_0$ is now explicitly treated as variable. Again, the linearity of L in $\tilde{\psi}_1$ and ψ_2 implies that these functions attain only the values 0 and a. In particular $\psi_2=0$, since ψ_2 has to be continuous. On the other hand, $\tilde{\psi}_1$ may have (at most) two jumps between 0 and a, occurring at the roots of the first variation of L with respect to $\tilde{\psi}_1$,

$$\begin{aligned} \operatorname{Im}\Big\{ & (1+\lambda_d-\lambda_A)\cdot\varphi(t-w_1)-\lambda_d\varphi(t-w_2) \\ & +\sum_{k=1}^{2}\lambda_k\varphi'(t-w_k)/g_k'\Big\}+\pi\lambda_0=0 \end{aligned} \tag{3.2}$$

Let these roots be γ_1 and γ_2 with $0\leqq\gamma_1\leqq\gamma_2\leqq\pi$, i.e.,

$$\tilde{\psi}_1(t)=\begin{cases} 0, & 0\leqq t\leqq\gamma_1 \\ a, & \gamma_1\leqq t\leqq\gamma_2 \\ 0, & \gamma_2\leqq t\leqq\pi \end{cases} \tag{3.3}$$

Then Eq. (2.35) yields $b=(\gamma_2-\gamma_1)a/\pi$ and the mapping according to Eq. (2.33) using Eq. (2.27) is

$$p(w)=\frac{a}{\pi}\left\{-(\gamma_2-\gamma_1)\varphi(w)+\log\frac{\vartheta_1(\gamma_1-w)}{\vartheta_1(\gamma_2-w)}\right\} \tag{3.4}$$

The model consists of two halfplanes at $z=z_0$ with a horizontal strip in the gap and a plane at $z=A$. It includes as limiting cases the extreme models (A) and (C) of Fig. 2, which correspond to $\alpha=\infty$ and $\gamma_1=0$, $\gamma_2=\pi$, respectively. To determine the model parameters for a given data set h_1, h_2, d, and A, the slightly modified Lagrange function

$$\begin{aligned} L=\operatorname{Im}\Big\{ & -p_1+\lambda_d(p_2-p_1-d)+\lambda_A(p_1+ia-iA) \\ & +\sum_{k=1}^{2}\tilde{\lambda}_k(g_k'/p_k'-h_k)\Big\} \end{aligned} \tag{3.5}$$

is used, differing from Eq. (3.1) in that, instead of the data kernels for $1/h_k$, the kernels for h_k are considered. The reason for this is that the associated $\tilde{\lambda}_k$ has an immediate interpretation, since the Lagrangian multipliers measure the sensitivity of the objective function z_0 to small changes in the data (Luenberger 1969, p. 221).

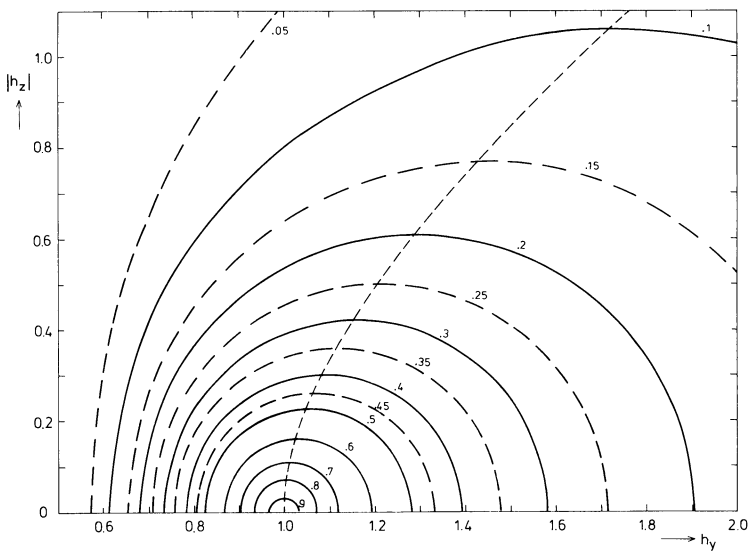

Fig. 4. Iso-lines for z_0/A (curve parameter) and the curve joining the maxima of the iso-lines. The latter curve is used if only h_z is given

In particular

$$\tilde{\lambda}_k=\frac{\partial z_0}{\partial h_{zk}}+i\,\frac{\partial z_0}{\partial h_{yk}},\qquad \mathrm{Im}\,\lambda_d=\partial_d z_0,\ \lambda_A=\partial_A z_0 \tag{3.6}$$

At an extremum, the partial derivatives of L with respect to real and imaginary part (if present) of the variables $\tilde{\lambda}_1$, $\tilde{\lambda}_2$, λ_d, λ_A, w_1, w_2, γ_1, γ_2, a and α have to vanish, yielding a system of fifteen equations (linear in the Lagrangian multipliers) for fifteen real unknowns. Also, Eq. (3.2) has to be satisfied for $t=\gamma_1, \gamma_2$, introducing λ_0 as an additional variable. It is easily verified that the two latter conditions and the conditions on the partial derivatives of L with respect to γ_1 and γ_2 provide only three independent equations, implying that Eq. (3.2) can be ignored (since λ_0 is of no interest).

As an example, for $h_1=(1.0,\ -0.5)$, $h_2=(1.5,\ 0.0)$ and $d/A=0.25$ we obtain

$$\tilde{\lambda}_1=(0.2113, 0.2672)\,A,\quad \tilde{\lambda}_2=(-0.1018,\ -0.0538)\,A$$
$$\lambda_d=(-0.3550, 0.3528),\quad \lambda_A=0.0694$$
$$w_1=(0.3387, 0.9118),\quad w_2=(2.9917, 1.1482)$$
$$\gamma_1=0.2389,\quad \gamma_2=2.3056,\quad a=0.8424\,A,\quad \alpha=3.8923$$

Hence, $z_0=0.1576\,A$. The abscissae of observation points and of halfplane and strip edges are, respectively, $-0.2241\,A$, $+0.0259\,A$; $-3.5008\,A$, $+1.1141\,A$; $-0.0623\,A$, $+0.0619\,A$. In a single-point extremum model h_1 and h_2 would yield $z_0/A=0.2213$ and 0.3376. This demonstrates that consideration of the field gradient can significantly improve the depth estimate. For different data, one might try to find the corresponding parameters by solving a sequence of problems, which gradually transform the above data into that required.

The doubly connected model breaks down if the solution of the system demands $\gamma_1<0$ or $\gamma_2>\pi$. In this case a triply connected model is required, where for $\gamma_1<0$ ($\gamma_2>\pi$) the two halfplanes at $z=z_0$ merge into a second strip to the right (left) of the first. It has not been possible to formulate the conditions under which a switch to triply connected conductors becomes necessary, in terms of the data. However, from

$$\partial_{\gamma_1} L=0\quad\text{or}\quad \partial_{\gamma_2} L=0$$

it is inferred that limiting models satisfy

$$\mathrm{Im}\,(\tilde{\lambda}_1 h_1+\tilde{\lambda}_2 h_2)=0 \tag{3.7}$$

Defining the vector

$$\mathbf{h}=(h_{y1}, h_{z1}, h_{y2}, h_{z2})\quad\text{and}\quad D=\mathbf{h}\cdot\nabla z_0(\mathbf{h})$$

Equations (3.7) and (3.6) imply that for limiting models $D=0$, i.e., at the corresponding magnetic field values the hyperplanes through the origin are tangential to the surface $z_0=\text{const}$. An analogue of condition (3.7) also holds for single-point problems, where it means that the switch from simply to doubly connected conductors occurs, where in Fig. 4 the lines through $(h_y, h_z)=0$ are tangential to the z_0-isolines, i.e., at $h_y=1$.

The two-point problem becomes particularly simple if A (and a) tends to infinity. In this case, the image of the plane $z=A$ reduces to a point, i.e., $\gamma_1\to\gamma_2(=\gamma)$ such that $b=(\gamma_2-\gamma_1)a/\pi$ remains finite. Expanding Eq. (3.4) at $\gamma=\gamma_1$ using Eq. (2.27),

$$p(w)=-b\{\varphi(w)+\varphi(\gamma-w)\} \tag{3.8}$$

The edges of the halfplanes ($v=0$) and of the strip ($v=\alpha/2$), defined by $p'(w)=0$, occur at $u=\gamma/2$ and $u=(\pi+\gamma)/2$. Knowing the type of the model, the extremal parameters for the data set h_1, h_2 and d can be inferred as follows:

The current flows in the same direction in halfplanes and the strip. This is obvious for physical reasons and can be deduced from

$$h_y(y, z_0)\,dy=g'(w)\,du>0\quad\text{for}\quad v=0\quad\text{and}\quad v=\alpha/2$$

(Eqs. (2.32), (2.30), (2.29)), implying that h_y is different in sign immediately above and below the conductors. Let $j(y)\geqq 0$ be the induced sheet-current density at $z=z_0$, normalized by H_n. Then the normalized magnetic field of internal origin at a surface point $p=y+iz_0$ is given by ($p_0=y_0$)

$$h(p)-\frac{1}{2}=\frac{i}{2\pi}\int_{-\infty}^{+\infty}\frac{j(y_0)\,dy_0}{p-p_0}$$

whence using Schwarz's inequality

$$\begin{aligned}|h_1-h_2|^2&=\frac{d^2}{4\pi^2}\left|\int_{-\infty}^{+\infty}\frac{j(y_0)\,dy_0}{(p_1-p_0)(p_2-p_0)}\right|^2\\&\leqq\frac{d^2}{4\pi^2}\int_{-\infty}^{+\infty}\frac{j(y_0)\,dy_0}{|p_1-p_0|^2}\cdot\int_{-\infty}^{+\infty}\frac{j(y_0)\,dy_0}{|p_2-p_0|^2}\\&=\frac{d^2}{4z_0^2}(2h_{y1}-1)(2h_{y2}-1)\end{aligned}$$

or

$$z_0\leqq\frac{\sqrt{(2h_{y1}-1)(2h_{y2}-1)}}{2|h_1-h_2|}\,d \tag{3.9}$$

Equation (3.9) provides an upper bound for z_0, where the equality sign holds for a line current. The upper bound is also attained if a uniform vertical magnetic field is added to the line current field. This field can be conceived as the magnetic field of induced currents in remote halfplanes at such a distance from the surface observation points that a uniform vertical field is observed.

The currents in the strip degenerate into a line current if $\alpha\to\infty$. In this limit Eq. (3.8) reduces to

$$p(w)=-b\{\cot w+\cot(\gamma-w)\} \tag{3.10}$$

The condition that the edges of the two halfplanes ($u=\gamma/2$ and $u=(\pi+\gamma)/2$), lying at

$$y=-2b\cot(\gamma/2)\quad\text{and}\quad y=+2b\tan(\gamma/2) \tag{3.11}$$

tend to $y=\pm\infty$ requires that $b\to\infty$, however in such a way that b/α is finite, ensuring according to Eq. (2.31) a finite total current in the strip. The latter limit implies, in view of Eq. (3.10), that at a point p (not at infinity) $v\to\infty$, leaving be^{-2v} finite. Hence, using Eq. (2.32) and taking all limits into account,

$$h(p)=\tfrac{1}{2}(1-i\cot\gamma)+\frac{ib}{\alpha p} \tag{3.12}$$

The first term is the inducing field, the second term the uniform vertical field from the induced currents in the remote halfplanes, and the third term the field of an induced line current at the origin of strength I, given by Eq. (2.31). A simple relationship between γ and the ratio of the distances to the edges of the halfplanes can be established by Eq. (3.11). By means of Eq. (3.12) for $p=p_1$ and $p=p_2$ the five parameters z_0, γ, b/α, y_1, and y_2 are easily adjusted to the five data h_1, h_2, and d. In particular, as expected,

$$z_0=\frac{\sqrt{(2h_{y1}-1)(2h_{y2}-1)}}{2|h_1-h_2|}\,d \tag{3.13}$$

Equation (3.13) assigns a depth z_0 to any data set, even if inconsistent (e.g., $h_{y1}=0.5$, $h_{y2}>0.5$) or pathologic ($h_{y1}=h_{y2}$, $h_{z1}>h_{z2}$, where $y_1\to\pm\infty$ for $h_{y2}=h_{y1}\mp 0$).

Although it is appealing that Eq. (3.13) depends on measurable data only, the absence of a priori assumptions renders it inefficient.

Finally, a comment on the triply connected domain with two horizontal strips at $z=z_0$, which is necessary for $\gamma_1<0$ or $\gamma_2>\pi$. Although the mapping is no longer univalent in this case, the value obtained for z_0 will still be very reliable, as in the single-point problem. As an alternative we may try to adjust the parameters of the model (of known type) by direct model calculations. For a sheet-current density $j(y)$ at $z=z_0$ the magnetic field is

$$h(p)=1+\frac{i}{2\pi}\int_{-\infty}^{+\infty}\left\{\frac{1}{p-y_0}-\frac{1}{p-(y_0-2ia)}\right\}j(y_0)\,dy_0 \tag{3.14}$$

The second term in the integral is the mirror image of j at $\mathrm{Im}\,p=-a$, where the imaginary part of the complex potential $f(p)$ has to vanish. Hence,

$$f(p)=p+ia+\frac{i}{2\pi}\int_{-\infty}^{+\infty}\log\left\{\frac{p-y_0}{p-y_0+2ia}\right\}j(y_0)\,dy_0$$

The condition $\mathrm{Im}\,f(p)=0$ for $y\in C$, where C is the union of conductors at the level $z=z_0$, then leads to the integral equation

$$a+\frac{1}{4\pi}\int_{-\infty}^{+\infty}\log\left\{\frac{(y-y_0)^2}{(y-y_0)^2+4a^2}\right\}j(y_0)\,dy_0=0,\qquad y\in C \tag{3.15}$$

which is easily solved, particularly if the edge singularities of j in a strip from y_1 to y_2 are isolated by assuming

$$j(y)=\tilde{j}(y)/\sqrt{(y_2-y)(y-y_1)},\qquad y\in(y_1,y_2)$$

4 An Application

In cooperation with U. Schmucker, parts of his magnetic field data collected during the IGY along north-south profiles across the North German conductivity anomaly (Schmucker 1959) have been reanalyzed with particular emphasis on the construction of a reasonable magnetic reference field (Weidelt 1978). Figure 5 presents the transfer functions h_y and h_z for a period of $T=1800$ s on the eastern profile. Of course, the out-of-phase component has to be ignored in the simple perfect conductor model.

The depth to the top of the anomalous conductivity causing this pronounced anomaly is most restricted by the magnetic fields at the three sites

GT (Göttingen): $h(\mathrm{GT})=(0.69,\,-0.20)$
FAL (Fallersleben): $h(\mathrm{FAL})=(1.06,\,-0.78)$
EBS (Ebstorf): $h(\mathrm{EBS})=(1.24,\,+0.07)$

at profile distances 99 km and 68 km apart.

First the two-point formula, Eq. (3.13) for $A=\infty$ is applied. The depth z_0 can be obtained for any two points of the profile. However, only the *smallest* value obtained is of geophysical interest. The pair FAL-EBS yields $z_0=50$ km and the pair GT-FAL $z_0=47$ km.

For more useful estimates we have to fix the depth A, which in the real geophysical situation can be approximately identified with a regional average of

$$\mathrm{Re}\,\{E_x(\omega)/(i\omega\mu_0 H_y(\omega))\}$$

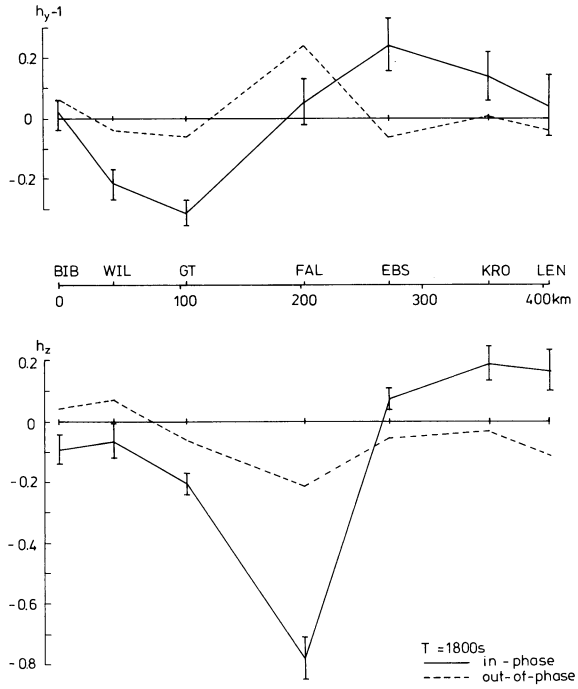

Fig. 5. Transfer functions and their standard variations on the eastern profile across the North German conductivity anomaly

for the frequency $\omega=2\pi/T$ (Schmucker 1970), where E_x is the horizontal electric field perpendicular to H_y. Taking $A=200$ km, the site FAL is the most restricting for the single-point problem, yielding according to Fig. 4 $z_0=24$ km. To a minor extent, the depth is also restricted by the low h_y(GT)-value ($z_0=34$ km).

Proceeding to two-point problems with finite A, the stations FAL-EBS reduce z_0 to 22 km, and the sites GT-FAL reduce it even further to 17.7 km. In the latter case the extremal model consists at the level z_0 of a conducting strip between 18 km and 133 km north of FAL and two remote halfplanes with edges 431 km south and 719 km north of FAL and of a conducting plane at the level A. The Lagrange multiplier $\lambda_A=0.05$ indicates that an increase of the poorly known depth A by 50 km (say) would increase z_0 by about 2.5 km.

It should be emphasized that the actual extremal model, which fits only a few data, is not of great interest. The only relevant information is the number $z_0=17.7$ km, meaning that any two-dimensional perfect conductor model with $A=200$ km explaining the data will show a conductor shallower than z_0. The data errors introduce into z_0 an uncertainty of at most ± 5.6 km, as can be deduced from $\tilde{\lambda}_1$ and $\tilde{\lambda}_2$.

5 Conclusions

The extremal models, which have been constructed for $N=1$ or 2 observation points, consist of a conducting plane at a given depth $z=A$ and either N gaps or N conducting strips at the level $z=z_0$. Apart from transition models, strips and gaps are of finite lateral extent. Including z_0, the coordinates of the edges with respect to the observation points are specified by $2N+1$ real constants. $2N$ equations are furnished by the data and the last by an extremal condition (not given explicitly for $N=2$).

The above results can be generalized to arbitrary N, yielding an M-connected conductor ($M=N$ or $N+1$). The exterior of the conductors is mapped by a univalent mapping onto the exterior of M parallel slits with pre-assigned inclination to the real axis (Goluzin 1969, pp. 210, 275). Although some insight into the general structure of the problem is obtained by considering arbitrary N, the problem is not open to simple numerical treatment. However, knowing the structure of the extremal model, the problem may be handled by Eqs. (3.14) and (3.15): Pre-assigning a small value of z_0, we try to infer the $2N$ edge coordinates from the $2N$ data, which is a nonlinear problem. If a set of coordinates can be found, z_0 is gradually increased until a solution is no longer obtained. The limiting value of z_0 will be considered as the best possible estimate.

A more urgent need than the generalization to arbitrary N is the generalization to conductors of finite conductivity, incorporating the out-of-phase component of the transfer functions into rating the out-of-phase component of the transfer functions into the data. These models will certainly considerably improve the depth estimate. Although the above results may serve as guidelines, the method of solution must be quite different from that presented here. Perhaps the method of analytic continuation of electromagnetic fields, as developed by Zdhanov (1980), may turn out to be quite useful.

Acknowledgements. I would like to thank the two referees for their helpful criticism.

References

Abramowitz, M., Stegun, I.A.: Handbook of mathematical functions. New York: Dover Publications 1965

Barcilon, V.: Ideal solution of an inverse normal mode problem with finite spectral data. Geophys. J.R. Astron. Soc. **56**, 399–408, 1979

Bott, M.H.P., Smith, R.A.: The estimation of the limiting depth of gravitating bodies. Geophys. Prospect **6**, 1–10, 1958

Goluzin, G.M.: Geometric theory of functions of a complex variable. Transl. Math. Monographs, Vol. 26. Providence: Amer. Math. Soc. 1969

Huestis, S.P.: Extremal temperature bounds from surface gradient measurements. Geophys. J.R. Astron. Soc. **58**, 249–260, 1979

Koppenfels, W.v., Stallmann, F.: Praxis der konformen Abbildung. Grundlehren Math. Wiss., Vol. 100. Berlin: Springer 1959

Luenberger, D.G.: Optimization by vector space methods. New York: Wiley 1969

Parker, R.L.: Inverse theory with grossly inadequate data. Geophys. J.R. Astron. Soc. **29**, 123–138, 1972

Parker, R.L.: Best bounds on density and depth from gravity data. Geophysics **29**, 123–138, 1974

Parker, R.L.: The theory of ideal bodies for gravity interpretation. Geophys. J.R. Astron. Soc. **42**, 315–334, 1975

Rietsch, E.: Extreme models from the maximum entropy formulation of inverse problems. J. Geophys. **44**, 273–275, 1978

Sabatier, P.C.: Positivity constraints in linear inverse problems, parts I and II. Geophys. J.R. Astron. Soc. **48**, 415–469, 1977a, b

Sabatier, P.C.: On geophysical inverse problems and constraints J. Geophys. **43**, 115–137, 1977c

Safon, C., Vasseur, G., Cuer, M.: Some applications of linear programming to the inverse gravity problem. Geophysics **42**, 1215–1229, 1977

Schmucker, U.: Erdmagnetische Tiefensondierung in Deutschland 1957/59: Magnetogramme und erste Auswertung. Abh. Akad. Wiss. Göttingen, Math.-Phys. Kl. Beitr. z. IGJ, Heft 5, 1959

Schmucker, U.: Anomalies of geomagnetic variations in the southwestern United States. Bull. Scripps Inst. Oceanogr. **13**, 1–165, 1970

Smith, R.A.: Some depth formulae for local magnetic and gravity anomalies. Geophys. Prospect **7**, 55–63, 1959

Smith, R.A.: Some formulae for interpreting local gravity anomalies. Geophys. Prospect **8**, 607–613, 1960

Weidelt, P.: Entwicklung und Erprobung eines Verfahrens zur Inversion zweidimensionaler Leitfähigkeitsstrukturen in E-Polarisation. Habilitationsschrift, Math.-Nat. Fak. Univ. Göttingen 1978

Whittaker, E.T., Watson, G.N.: A course of modern analysis, 4th edn. London: Cambridge University Press 1927

Zdhanov, M.S.: Cauchy integral analogues for the separation and continuation of electromagnetic fields within conducting matter. Geophys. Surv. **4**, 115–136, 1980

Received October 23, 1980; Revised Version January 27, 1981
Accepted January 27, 1981